Figure S1. KEGG pathway enrichment analyses and mass spectrometry peak of YBX1. (A) KEGG pathway enrichment analyses according to P-value. (B) Mass spectrometry peak of YBX1. KEGG, Kyoto Encyclopedia of Genes and Genomes; YBX1, Y-box binding protein 1.

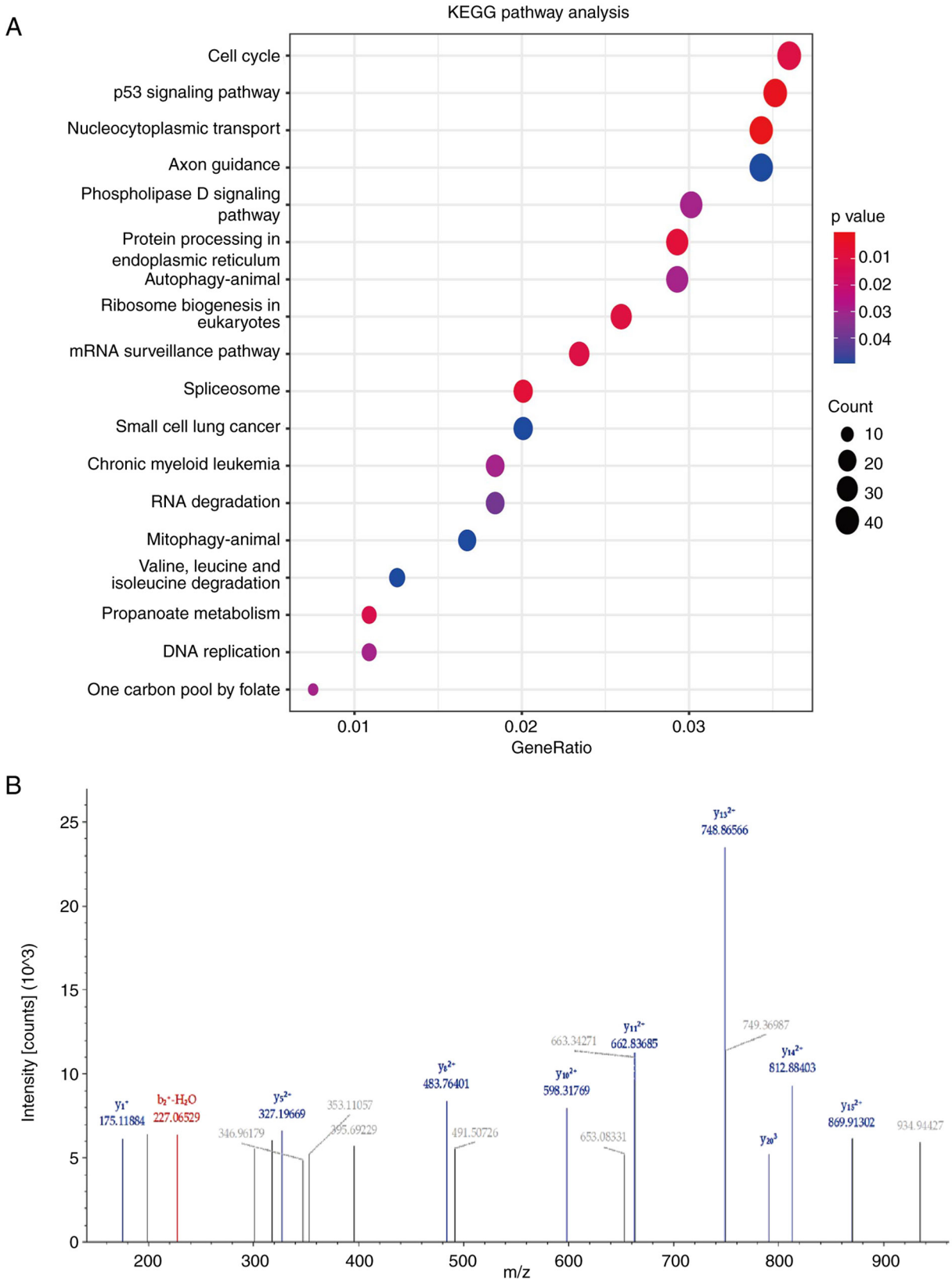

Figure S2. Validation of YBX1 transfection efficiency. YBX1 expression levels were detected using western blotting when it was knocked down or overexpressed in LNCaP and 22Rv1 cells. **P<0.01 vs. the si-NC group; #P<0.05 vs. the vector group. NC, negative control; OE-YBX1, YBX1 overexpression plasmid; si, small interfering; YBX1, Y-box binding protein 1.

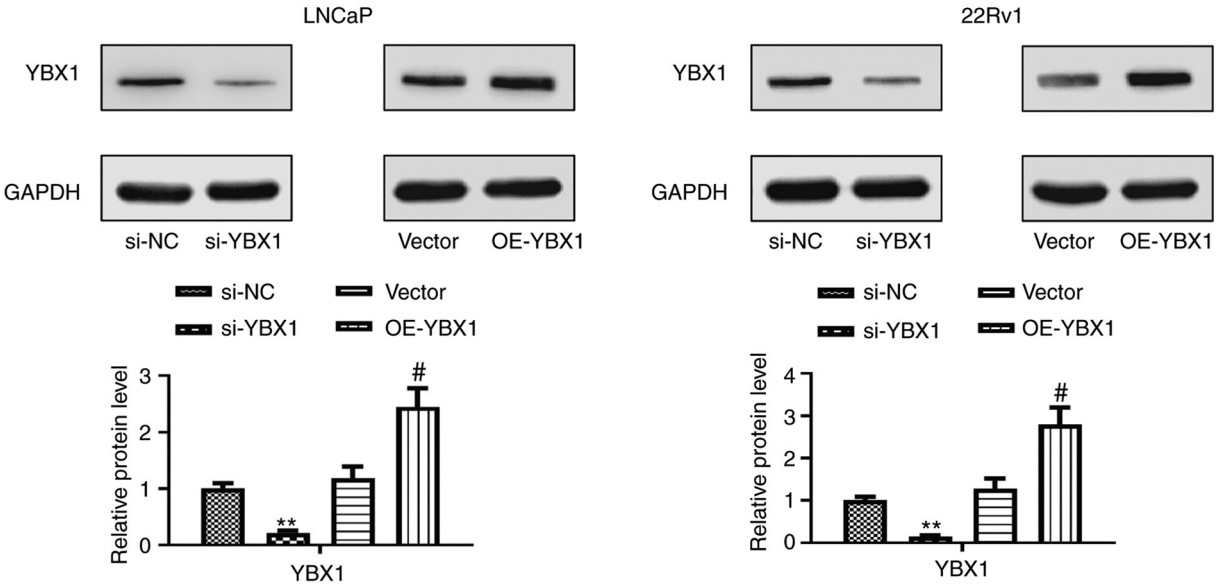

Figure S3. Characteristics of PBAE. (A) Cell Counting Kit-8 results confirmed that PBAE exhibited no obvious toxicity at different concentrations in LNCaP and 22Rv1 cells. (B) PBAE loading efficiency. (C) Transmission electron microscopy image of PBAE/si-CASC11 nanocomplexes. Scale bar, 200 nm. (D) Distribution of PBAE/si-CASC11 nanocomplexes in terms of size. (E) Relative expression levels of CASC11 in different groups. **P<0.01. CASC11, cancer susceptibility candidate 11; PBAE, poly (β-amino ester); si, small interfering.

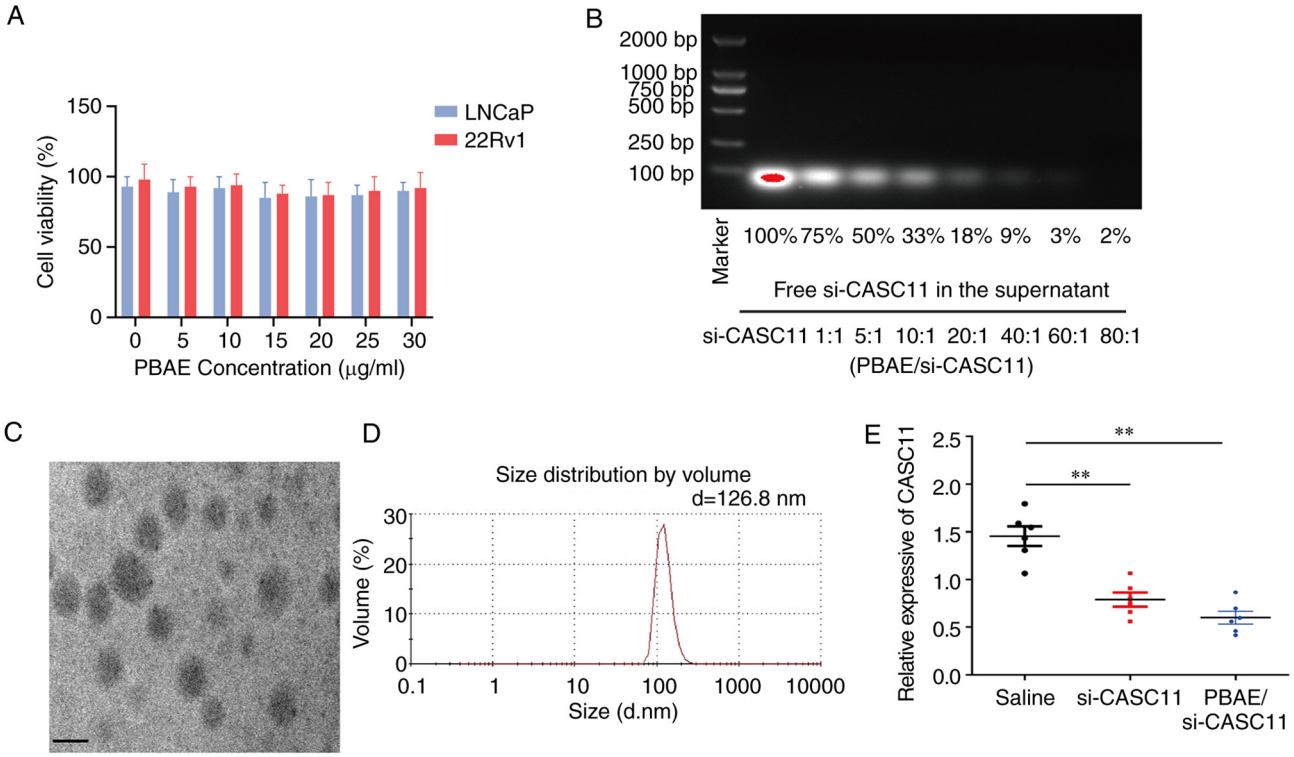

Figure S4. Hematoxylin and eosin staining images of the liver and kidney revealed that no notable morphological changes occurred in the groups. Scale bar, 200 μm. CASC11, cancer susceptibility candidate 11; PBAE, poly (β-amino ester); si, small interfering.